SOME RECENT OBSERVATIONS ON STEAM GENERATOR TUBING DEGRADATION

Gabriel Ogundele, Malcolm Clark, Guylaine Goszczynski, Amy Lloyd,
Kinectrics Inc.
Sandra Pagan,
Ontario Power Generation
Ken Sedman,
Bruce Power
Peter King,
Babcock & Wilcox Canada

ABSTRACT

The steam generator tubing materials at the Pickering, Bruce, and Darlington nuclear stations are manufactured from UNS Alloy N04400, UNS Alloy N06600, and UNS Alloy N08800, respectively. These materials are subjected to different operating conditions. This paper presents a summary of the recent damage mechanisms observed on the inside and outside surfaces of the tubes (based on the metallurgical examination of removed tubes). The mechanisms that have been observed include underdeposit pitting, stress corrosion cracking, intergranular attack, fretting, and erosion corrosion. In addition, the morphology of the flaws and, where possible, the likely causative factors are discussed.

INTRODUCTION

The CANDU (Canadian Deuterium Uranium) pressurized heavy water reactors in Ontario are operated by Ontario Power Generation (Darlington, Pickering A, and Pickering B) and Bruce Power (Bruce A and Bruce B). The operating parameters of the steam generators (SG) at each of the stations are presented in Table 1 [1]. The SGs are vertical, recirculating, U-tube heat exchangers. The steam generator tubing materials at these stations are manufactured from Monel 400 (UNS Alloy N04400) for Pickering A and B, Inconel 600 (UNS Alloy N06600) Bruce A and B, and Incoloy 800 (UNS Alloy N08800) for Darlington. As evident in Table 1, these units are subjected to different operating conditions. The nominal ASME and specified CANDU chemical compositions of these alloys are presented in Tables 2 and 3 respectively. The SG tubing materials have experienced a variety of degradation modes; some of which are documented in a number of publications [2-6]. The location of some of these degradation modes are summarized in Figure 1 [5]. This paper presents some previous and recent flaws observed on the inside and outside surfaces of removed tubes. The information was gathered from results of numerous failure analyses of removed tubes using techniques described elsewhere [7].

Table 1: Some Design Characteristics of Canadian CANDU Plants Steam Generators [1]

	Pickering A	Pickering B	Bruce A	Bruce B	Darlington
No. of units	4	4	4	4	4
Net capacity (MWe)	515	515	760	840	880
No. SG/Reactor	12	12	8	8	4
No. Tube/SG	2600	2573	4200	4200	4663
SG Tube Material	UNS N04400	UNS N04400	UNS N06600	UNS N06600	UNS N08800
SG Tube Size	12.7mm OD 1.11mm wall thickness	12.7mm OD 1.11mm wall thickness	12.7mm OD 1.11mm wall thickness	12.7mm OD 1.11mm wall thickness	12.7mm OD 1.11mm wall thickness
Support Structure	Lattice Bars	Broached Trifoil Holes	Broached	Broached	Lattice Bars

			Trifoil Holes	Trifoil Holes	
Support Structure	Cu-bearing Steel	Carbon steel	Carbon steel	Carbon steel	410 SS
Preheater	Integral	Integral	Separate	Separate	Integral
Hot Leg Temp. ^{o}C	293	290	304	304	309
Cold Leg Temp.^{o}C	249	249	265	265	265
Feedtrain Material	Mixed Fe/Cu (partial Cu replacement)	All ferrous (copper replaced)	Mixed Fe/Cu	All Ferrous	All Ferrous
Water Chemistry Control	All Volatile (Morph/N_2H_4)	All Volatile (Morph/N_2H_4)	All Volatile (Morph/N_2H_4)	All Volatile (Morph/N_2H_4)	All Volatile (NH_3/N_2H_4)
Commercial Operation	U1 July '71 U2 Dec '71 U3 June '72 U4 June '73	U5 May '83 U6 Feb '84 U7 Jan '85 U8 Feb '86	U1 Sept '77 U2 Sept '77 U3 Feb '78 U4 Jan '79	U5 Mar '85 U6 Sept '84 U7 Apr '86 U8 May '87	U1 Nov '92 U2 Oct '90 U3 Feb '93 U4 Jan '93

Table 2: Nominal (ASME) Chemical Composition of the Alloys

Element	**Specification**		
	Monel 400	Inconel 600	Incoloy 800
C	0.30 max	0.15 max	0.10 max
Al	-	-	0.15-0.60
Si	0.50 max	0.5 max	1.0 max
S	0.024 max	0.015 max	0.015 max
Ti	-	-	0.15-0.60
Cr	-	14.0-17.0	19.0-23.0
Mn	2.0 max	1.0 max	1.50 max
Fe	2.5 max	6.0-10.0	39.5 min
Ni	63.0 – 70.0	72.0 min	30.0-35.0
Cu	28.0-34.0	0.5 max	0.75 max

Table 3: Specified Chemical Composition of SG Tubing Materials for CANDU Plants

Element	**Specification**		
	Pickering* UNS Alloy N04400	Bruce UNS Alloy N06600	Darlington UNS Alloy N08800
C	0.085 (0.081)	0.03 max	0.03 max
Mg	0.013 (0.013)	-	-
Al	0.102 (0.106)	-	0.15-0.45
Si	0.12 (0.16)	0.5 max	0.75 max
P	-	0.015 max	-
S	0.001 (0.001)	0.015 max	0.01 max
Ti	-	-	0.35 min
Cr	0.01 (0.01)	14.0-17.0	21.0-23.0
Mn	1.07 (1.08)	1.0 max	1.0 max
Fe	1.25 (1.27)	6.0-10.0	Remainder
Co	-	0.015%	-
Ni	64.59 (64.40)	72.0 min	32.5-35.0
Cu	32.70 (32.18)	0.5 max	0.75 max
N	-	0.05 max	-
Ti/C	-	-	12 min
Ti/(C+N)	-	5 min	8 min

*Specification for Pickering tubing mill certificate analysis (Check Analysis)

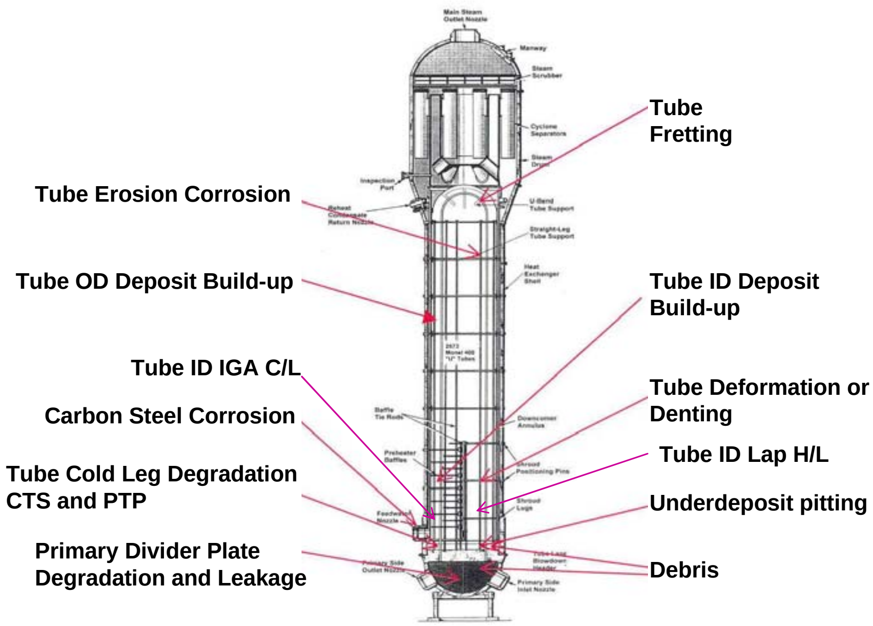

(a) Steam generator design at OPG stations

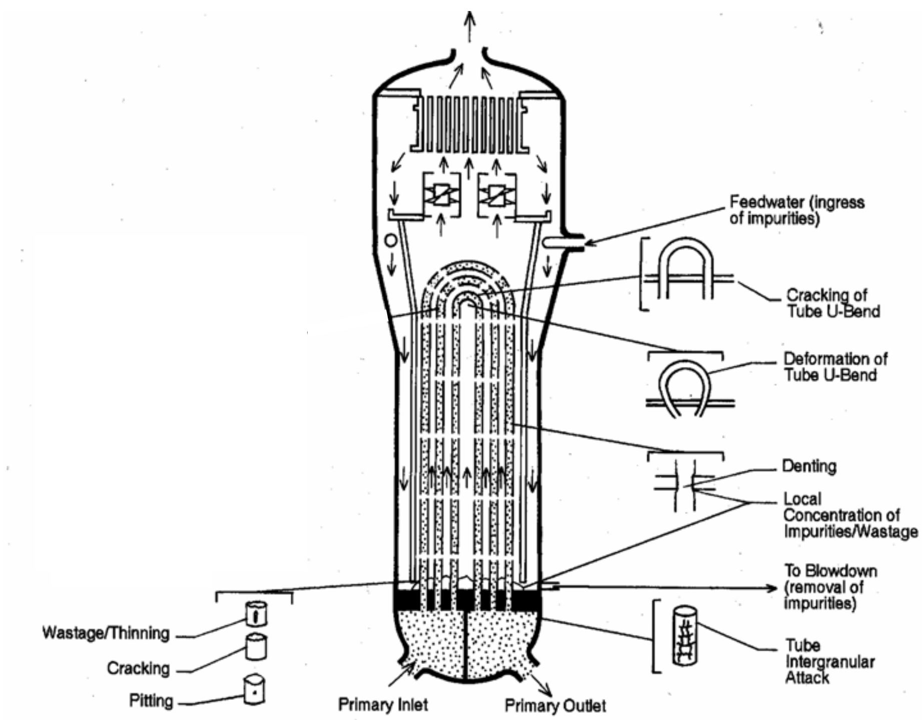

(b) Steam generator design at Bruce Power station

Figure 1: Locations of degradation mechanisms observed in CANDU Steam Generators

DEGRADATION MECHANISMS

Pitting and Underdeposit Corrosion

<u>Alloy 400:</u> For many years, the main type of degradation observed in Alloy 400 was underdeposit pitting corrosion that initiates from the outside surface of the tube [5]. Figure 2 shows some pitting corrosion degradation observed on the outside surface of the alloy. The pitting occurred mostly just above the upper rolled joint. In general, the degradation was characterized by wide-mouthed, dish shaped pits with a low aspect ratio, with no undercutting at the tube surface. Analysis of the deposits inside and around partial through-wall pits revealed the presence of chloride and sulfur ions. This is indicative of the presence of an environment conducive to underdeposit pitting. The likelihood of the initiation or growth of pits is dependent on the presence or absence of oxidizing species during SG operation. Layers of metallic Cu and metal oxides were observed in the sludge pile deposits and in some pits. This indicates that there was a cyclical variation in the oxidation potential during the SG operational cycle particularly during start-ups when higher levels of dissolved oxygen are present in the SG.

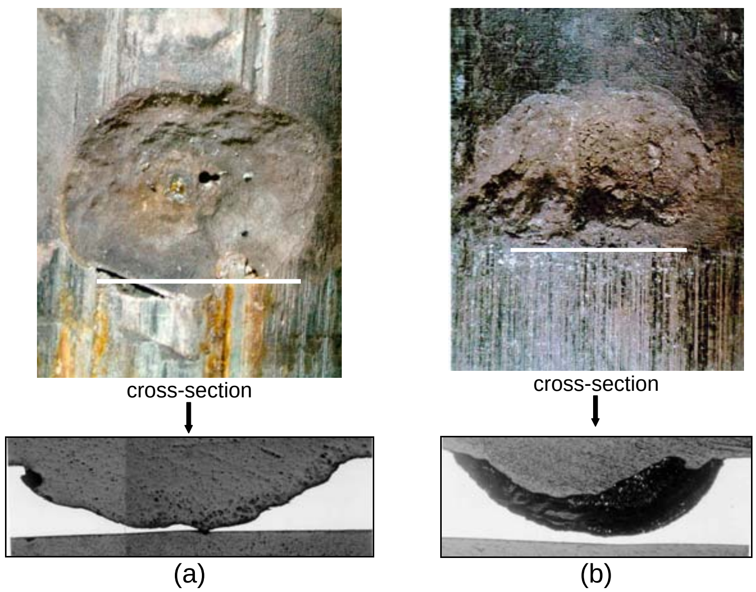

Figure 2: Pitting corrosion on Alloy 400; the pits are located just above the upper end of the rolled joint represented by the white horizontal line

<u>Alloy 600:</u> Figure 3 shows the nature of pitting corrosion observed on the outside surface of Alloy 600 tubing. The micro-pitting was usually associated with circular stains. The deposits in the pitted region were subjected to EDS (energy dispersive spectroscopy) analysis to determine the elemental composition. The general deposits contained contaminants commonly found in the secondary side tube deposits: Al, Si, S, Cl, and Ti. High Fe contents were observed (above that in the base metal). This indicated that the deposits likely contained magnetite. Two of the locations directly over the pits contained unusually high Cl contents but less Fe than in the general pit deposit. This finding strongly suggests that chloride ion played a significant role in the pitting process.

(a) pit on the outside surface (b) SEM image of the bright spot in ‘a’

Figure 3: Details of shiny pit showing optical micrographs and SEM micrographs of the pit center with crystallographic features and etched grain boundaries

<u>Alloy 800:</u> More recently, shallow pitting corrosion was observed on the outside surface of Alloy 800. The shallow wall loss, 10% through-wall (tw), appears to have occurred as a result of uniform localized corrosion rather than from a mechanical process.   Figure 4 shows the degradation just above a tube support. Preliminary evaluation of this degradation suggests that the affected SG tube material may contain some unique characteristics. The most significant finding from the material characterization was the titanium concentration which might have affected the corrosion resistance.

(a) outside surface of the tube

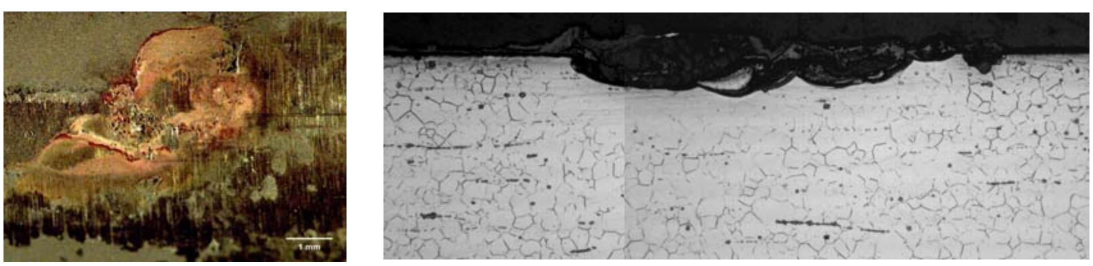

(b) pitted region (c) cross-section through the pit

Figure 4: Pitting in Alloy 800

Erosion-Corrosion

This mechanism has only been observed in Alloy 400 tubing. Figure 5 shows the outside surface of Alloy 400 that corroded due to erosion-corrosion. No erosion-corrosion degradation exceeding 20% tw has been observed from the first detection in 1997 to the present. This mode of degradation was initially observed to be most significant on the hot-leg side at the upper support plates in regions of high fluid flow during plant operation; but other SGs were also affected at the lower support plates [8-9]. The wall loss was present in the three flow holes (lobes) of the broached support plates and typically extended from the lower edge of the tube support to beyond its upper edge. Figure 6a shows typical surface characteristics of a fully developed feature with light deposits lodged in the groove of the facets created by the erosion-corrosion mechanism. This type of flaw is also called a “top hat” (TH) due to the overall physical characteristics of the degradation.

Light erosion corrosion feature at 1st Support

Moderate erosion corrosion feature at 3rd Support

Fully developed erosion corrosion feature at 8th Support

(a) Features at the supports

Cleaned surface at the affected region

Close-up view of the affected region

(b) View of an affected region on the tube surface

Figure 5: Morphology of erosion-corrosion degradation on the outside surface of Alloy 400

Cold Leg Thinning

Some general wall thinning has also been observed on Alloy 400 SG tubing. Figure 6 shows the nature of the degradation observed on the outer diameter surface of a tube removed from the cold leg region of the steam generator. This degradation occurred as volumetric wall loss (thinning) on the outside surface of the tube around the circumference and was associated with the support intersections (preheater section) or at the tubesheet [5]. The wall loss at the top of tubesheet ranged between 9% and 11%tw. There was no appreciable deposit at the support locations but there was evidence of patchy bright areas. Scanning electron microscopy (SEM) examination revealed general corrosion and minor intergranular (IGA) in these areas. No evidence of pitting or stress corrosion cracking was found in any of the corroded areas. The cause of this mode of degradation is not well understood.

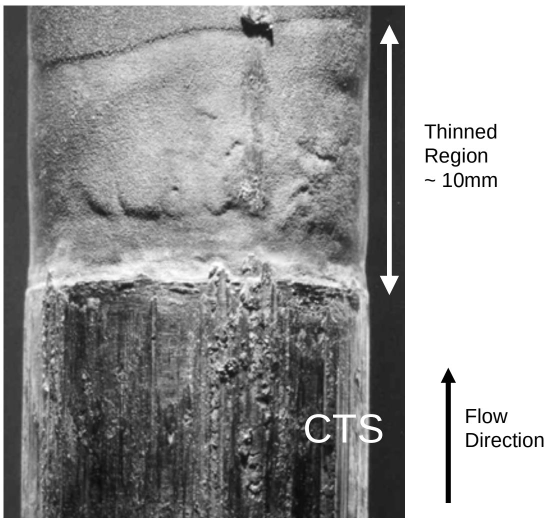

(a) affected region on the outside surface

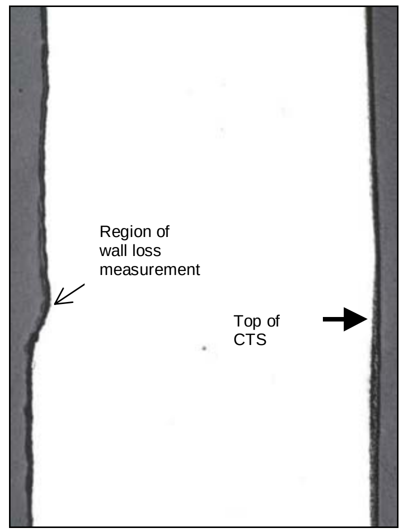

(b) cross-section

Figure 6: Wall thinning in Alloy 400 (a) outside surface, (b) Axial cross-section through the flaw

Intergranular Attack (IGA)

<u>Alloy 400:</u> Figure 7 shows typical characteristics of an area affected by IGA on the primary heat transport (PHT) “pure” heavy water side surface of Alloy 400 on the cold leg side. The flaws are characterized by a localized surface deposits with possible penetration through the thickness. Before destructive examination, the deposit (Figures 7a,c,e) were analysed and were found to consist mainly of Ni and Cu with Fe in the centre. Figures 7b,d show the transverse cross-sections revealing the extensive IGA morphology. The axial cross-section in Figure 7f revealed a larger axial subsurface extent. Metallic copper platelets were seen within the grain boundaries in the IGA region. As this type of degradation had not been previously observed on the Alloy 400 SG tubes, the flaw was subjected to further analyses using orientation imaging microscopy (OIM) to determine if there are strain concentrations along the IGA front. From the OIM analysis, no coherent strain field existed beneath the IGA front. Accordingly, there was no basis to suggest that these defects would lead to the nucleation and propagation of stress corrosion cracking (SCC). Though the damage displayed by the cross-sections was characteristic of IGA, the morphology, extent, and it’s presence on the inside surface is unusual in Alloy 400 from field experience and is considered to be most likely associated with historical primary side decontamination processes.

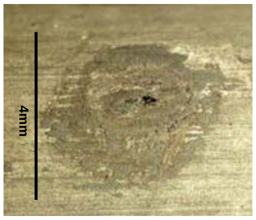

polishing direction

(a)

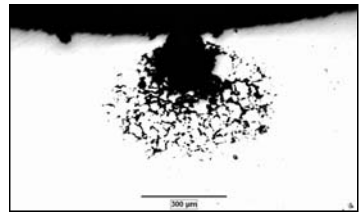

(b) transverse cross-section through ‘a’

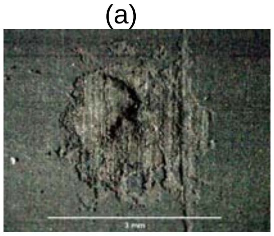

polishing direction

(c)

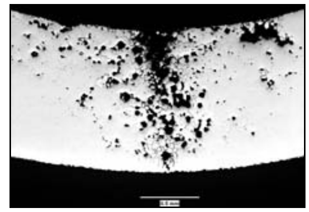

(d) transverse cross-section through ‘c’

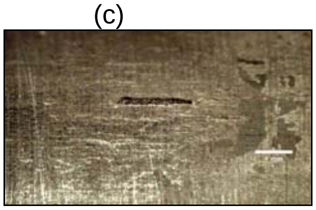

polishing direction

(e)

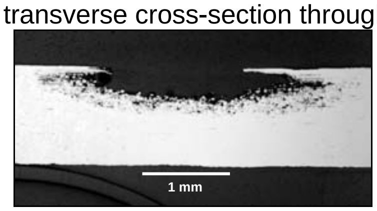

(f) axial cross-section through ‘e’

Figure 7: IGA patch on the inside surface of Alloy 400 (a,c,e) inside surface features, (b,d,f) cross-section through the flaw.

<u>Alloy 600:</u> Some localized outside surface flaws have been observed on Alloy 600 tubing. The flaws were found on the hot leg of the tube in the free span region. The outside surface of the tube and cross-section through such flaws can be seen in Figures 8 and 9. The indications were found to originate from oval or circular shaped patches of intergranular attack (IGA) located between 10 and 22 mm above the top of the tubesheet (Figure 8) and at the tubesheet (Figure 9). The orientation imaging microscopy (OIM) analysis conducted on the flaws indicated that the IGA propagated without any strain accumulation at the interfaces or along the crack-like features within the IGA patches. This observation suggests propagation of the IGA patch *<u>in advance</u>* of the crack-like features. The presence and location of the IGA does not appear to be related to any anomalies in grain size or texture effects. Dynamic secondary ion mass spectroscopy (SIMS) results suggested that sulfur or sulfur bearing compounds likely had a role in the IGA in the steam generator tube. No other species that could cause localized corrosion of the tube were detected.

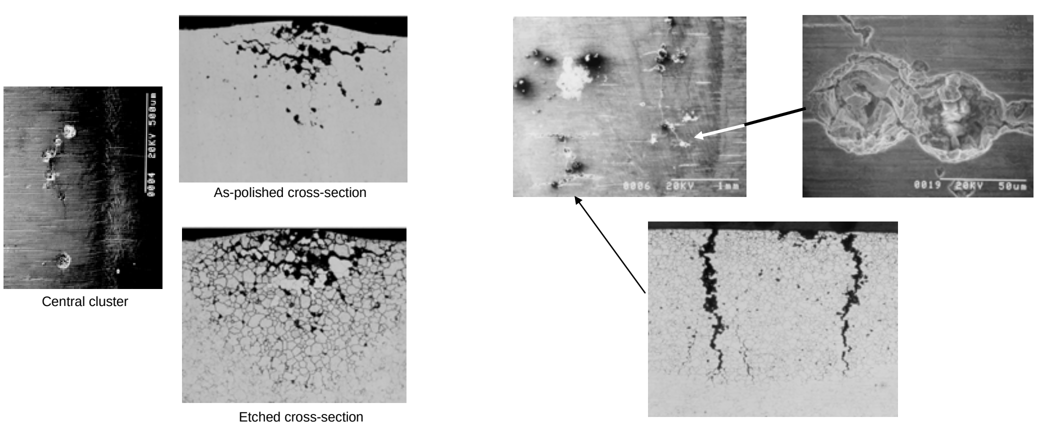

(a) (b)

Figure 8: IGA in Alloy 600 (a) transverse cross-section, (b) axial cross-section

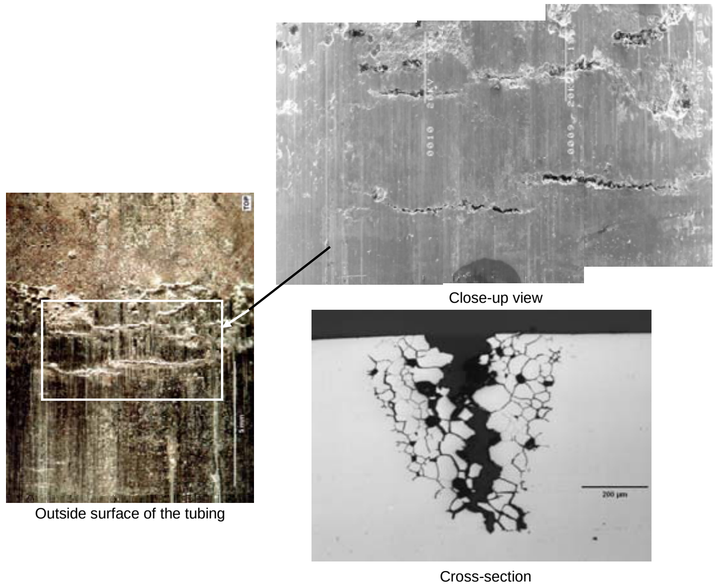

Figure 9: IGA in Alloy 600 with the transverse cross-section

Fretting Damage

Alloy 600: Figure 10 shows a fretting-type damage on the outside surface of Alloy 600. The fretting types of surface flaws are characterized as originating from the interaction of the tube and the broach plate land contact. This was aggravated by the tube support degradation in Unit 8.

Figure 10: Fretting damage on Alloy 600

Alloy 800: Tube fretting in the U-bend region, due to the interaction of the tubes with anti-vibration bar (AVB) support, has been observed at all Darlington steam generators [5]. Figure 11 shows the typical fretting feature found on the tube at the U-bend region. In the straight leg region, the fretting damage was much less severe and appeared different. The metallographic examination of Alloy 800 shows a region of fretting damage ("maple leaf" flaw) at the H04 support. As seen in Figure 12, the flaw consisted of very fine grooves that appear to be due to some type of mechanical micro-deformation process. The location at the bottom of the contact area with the lattice bars, suggested an interaction between the initial deposits and the lower edge of the bar producing this unusual deformation pattern. The features within and around the fine grooves do not suggest that they were produced by a flow-induced type of mechanism, gross mechanical deformation or steam cutting. The flaw is typical of a traditional fretting mechanism whereby fine metal particles removed by the mechanical movement of the tubes are oxidized and provide an abrasive surface for continual metal removal. This feature is similar to those observed on Alloy 600.

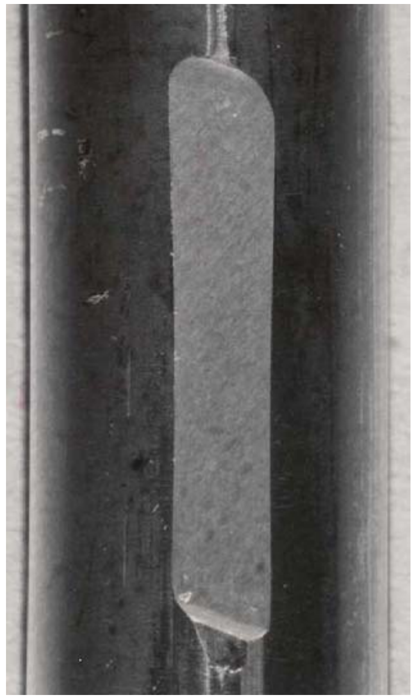

Figure 11: Fretting on Alloy 800 at U-bend support

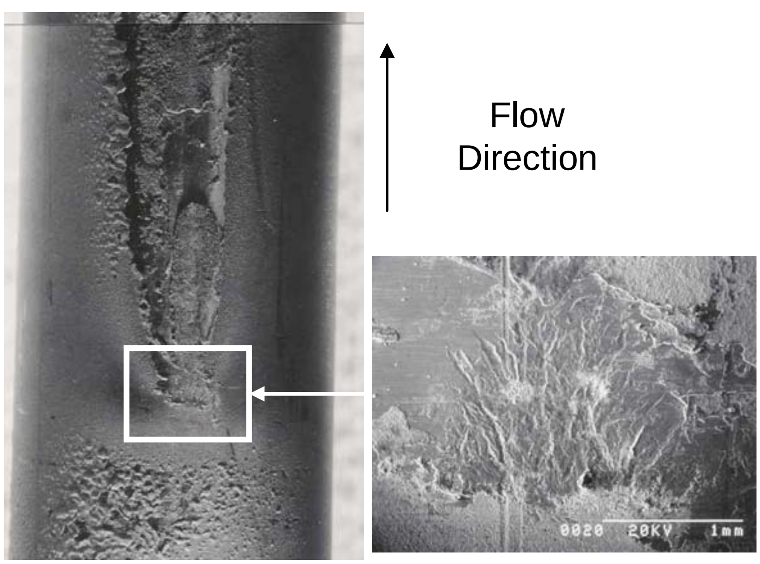

Figure 12: Fretting (maple leaf) damage on Alloy 800; right micrograph is an SEM image of the flaw

Outside Surface Stress Corrosion Cracking (ODSCC)

The steam generator tubing UNS Alloy N06600 (Alloy 600) suffered leaks at the U-bend region due to high cycle, low-stress amplitude fatigue cracking probably caused by flow-induced vibration [2] early in service life. Later, outside surface (OD) initiated circumferentially oriented stress corrosion cracking was also observed on the tubing (lead was implicated in the cracking process). In 1986, a lead shielding blanket inadvertently left in one of the steam generators dissolved in the secondary side water and exacerbated the SCC problem in one bank of boilers (U-bend cracking).

Top of Tubesheet Cracking

Some Alloy 600 tubing were observed to have experienced significant cracking in the roll transition zone (RTZ). These cracks were circumferential, OD initiated, and progressed in a fully intergranular manner as shown in Figure 13. The location of the cracking suggests that the cracking environment is formed inside the crevice between the tubesheet and the tube roll transition. Secondary side intergranular attack and stress corrosion cracking (OD IGA/SCC) in the upper roll transition region are the confirmed degradation mechanisms. Cracking is often accompanied by extensive intergranular attack and grain dropping around the main crack.

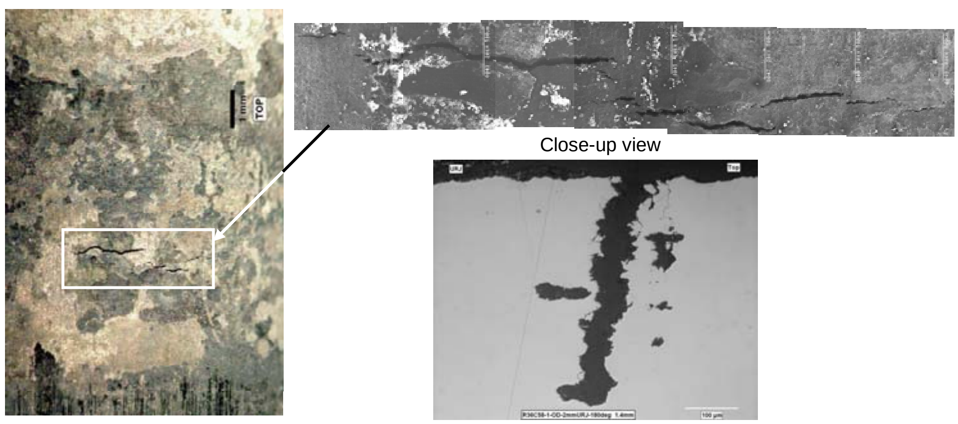

Figure 13: Circumferential cracking on the outside surface of Alloy 600

Environment Assisted Cracking in Alloy 400

An unusual type of degradation was observed on two Alloy 400 tubes. The observations indicated a crack-like flaw, which originated from the outside surface of a tube removed from the hot leg of a SG at Pickering NGS. The unusual characteristics of the degradation and ensuing analysis termed this degradation as a form of environment assisted cracking (EAC) that is non-classical in nature. This is because this type of morphology has not been reported elsewhere. The features did not display the characteristics of classical stress corrosion cracking (SCC) mechanism that generally includes multiple initiation sites and secondary branching. Figure 14 shows the feature as observed on the outside surface of the tube. The flaw was characterized as straight and axially oriented. Figure 15 shows the cross-section through a part of the flaw.

The pertinent parameters required for stress corrosion cracking (material/environment/stress factors) of Alloy 400 tubing material were individually examined. Based on the analyses, it was difficult to attribute the flaw to a typical stress corrosion cracking mechanism and as a consequence it would be more appropriate to define it as environmental assisted cracking (EAC) that likely initiated at a manufacturing defect (lap-type defect).

Stress corrosion cracking in UNS N04400 (Monel 400) is relatively rare, but there are documented cases in high pressure feedwater heaters from fossil-fired power stations with Monel 400 tubing operating in steam environments [10, 11]. The reported cracking was totally intergranular with some but not extensive side branching. Small parallel secondary cracks were sometimes reported. The crack appearances were similar to those seen in the present case with the exception of the apparent sideways intergranular corrosion of the crack surfaces (see Figure 17) and the lack of secondary cracking. The cracking in feedwater heaters was usually attributed to high residual stresses in the as-manufactured tubes (also absent in the present case) is not located in the rolled joint region but rather is in the free span.

Thus, from the current observations, it is not expected that the type of degradation found on Alloy 400 will take place in the absence of a lap-type defect.

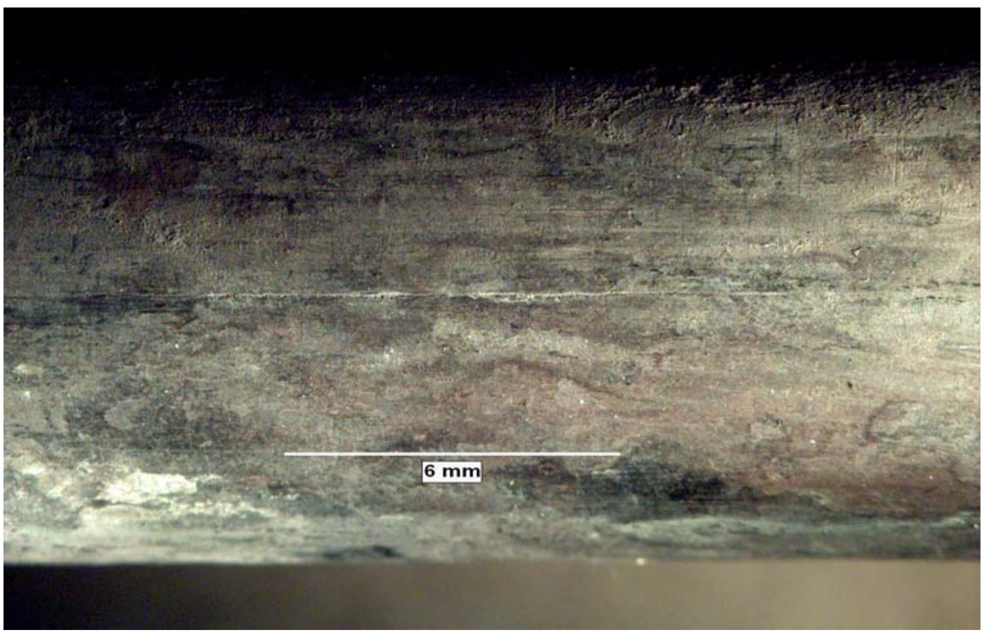

→ axial direction of the tube

Figure 14 Appearance of the flaw as visible on the OD and is oriented in the axial direction of the tube.

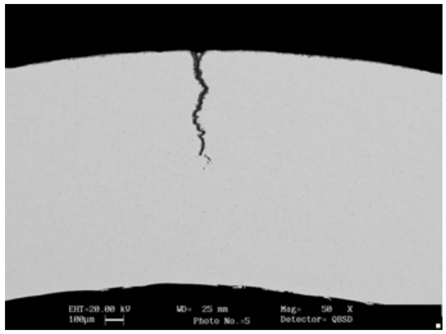

(a) transverse cross-section

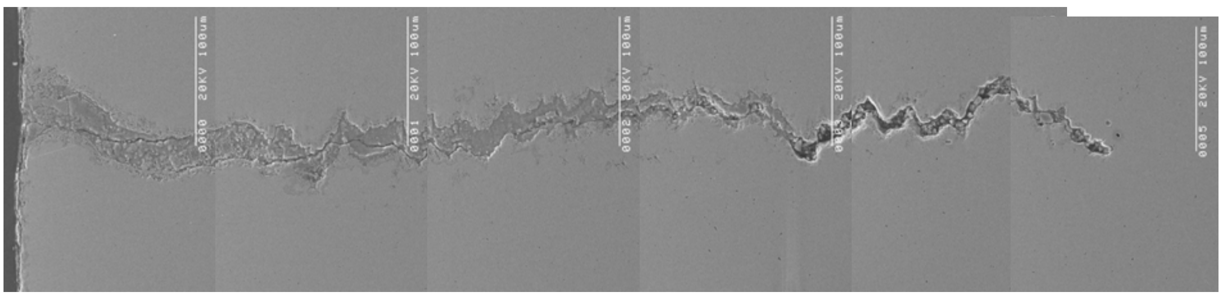

(b) SEM montage of the crack

Figure 15 Cross-section through a part of the flaw

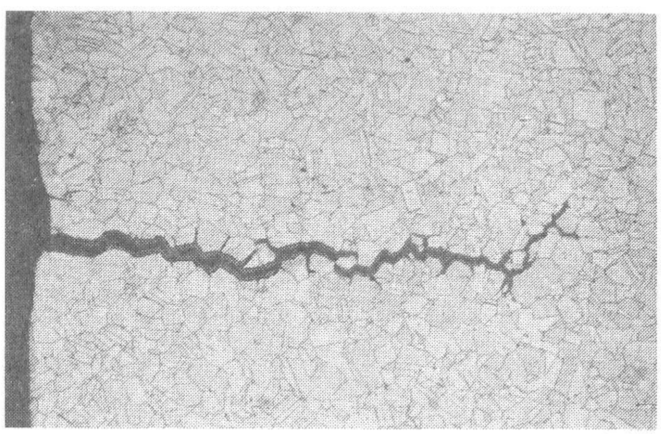

Figure 16 Cross-sectional views of cracking in Monel alloy 400 tubing from a high pressure feedwater heater [12]. This image is compared to that presented in Figure 15.

CONCLUSION

The steam generator tubing Alloys UNS Alloys N04400, N06600, and N08800 were selected as material of construction for CANDU applications on the basis of their strength and corrosion performance. The corrosion resistance will normally be imparted by a tenacious protective oxide layer on the material. In general, these materials would be expected to experience minimal general corrosion degradation. The extent of degradation by this general mechanism has been low with marginal or no measurable wall loss.

However, the degradation mechanisms highlighted above for these materials have been localized. The contributing factors ranges from upset chemistry, material imperfection, manufacturing defect, and mechanical influence. Following this, it is evident that Alloys N04400, N06600, and N08800 are susceptible to a variety of degradation mechanisms. The degradation mechanism in Alloy 800 have been the least, but the recent observation of underdeposit pitting in this Alloy is yet to be understood. As part of the life cycle management plans, CANDU operators, continue to carefully monitor and trend the degradations.

Metallurgical examination of removed tubes for investigation and assessment of new or existing degradation continues to form an important element of steam generator life cycle management plans.

REFERENCES

1. R. Dyck, P. Spekkens, K. Verma, and A. Marchand, “Operational Experience with Steam Generators in Canadian Nuclear Power Stations”, Proceedings of a Conference on Steam generator and Heat Exchangers, pp. 1-11 – 1-27, Toronto, 1990.

2. B. D. Warr, M. A. Clark and G. Bellamy, "Operating Experience and Laboratory Studies with Fatigue and Stress Corrosion Cracking of Inconel 600 Steam Generator Tubes at Ontario Hydro", ASM International, Paper 8517-016, Int. Conf. on Nucl. Power Plant Aging, San Diego, CA, 8-12 July, 1985.

3. J. Curcio and M. W. Shanahan, “Steam Generator Tube Performance in Ontario Hydro CANDU PHWRS”, Proc. Environmental Degradation of Materials in Nuclear Power Systems – Water Reactors, Eds. G. J. Theus and J. R. Weeks, TMS, pp. 409-417, 1988.

4. M. Clark, O. Lepik, A. Brennenstuhl, M. Mirzai, and I. Thompson, “Top of Tubesheet Cracking in Bruce NGS Steam Generator Tubing: An Assessment of Material and Environmental Factors”, Proc. of 9th Inter. Symp on Environmental Degradation of Materials in Nuclear Power Systems – Water Reactors, Eds., F. P. Ford, S. M. Bruemmer, and G. S. Was, TMS, pp. 629-636, 1999.

5. C. C. Maruska, “Steam Generator Life Cycle Management Ontario Power Generation 9OPG) Experience”, Presented at the 4th CNS International Steam Generator Conference, May 5-8, 2002.

6. G. Ogundele, M. Clark, G. Goszczynski, A. Lloyd, S. Pagan, K. Sedman, and P. King, “A Review of Some Degradation Mechanisms in CANDU Steam Generator Tubing”, Paper ICONE14-89859, Proceedings of ICONE14, 14th International Conference on Nuclear Engineering, July 17-20, Miami, Florida USA, 2006.

7. G. Ogundele, A. MacIntosh, M. Clark, and O.Yong, “Approach to Failure Analysis of Nuclear Steam Generator Tubing”, Paper 23-4, Presented at the 16th International Corrosion Congress, Beijing, China, September 19 – 24, 2005.

8. M. A. Clark, O. Lepik and T. Lau, “Erosion Corrosion Damage in Alloy 400 Steam Generator Tube from Pickering NGS”, Proc. of the Third Inter. Conf. on Steam Generators and Heat Exchangers, Canadian Nuclear Society, pp. 575-588, 1998.

9. G. Ogundele and A. Lloyd, “Erosion Corrosion of UNS Alloy N04400”, Presented at 12th International Conference on Environmental Degradation of Materials in Nuclear Systems-Water Reactors”, Salt Lake City, Utah, August 15-19, 2005.

10. Pement et al., “Microanalytical Characterization of Stress Corrosion Cracking in Power Plant Heat Exchanger Tubing”, Materials Performance, Jan 1977.

11. G. Bellamy, “Cracking of Monel Alloy 400 Tubing in *[a]* High Pressure Feedwater Heater – LVGS”, Unpublished Work.

12. M. D. Wright, G. Goszczynski and F. Peca, “Embrittlement of Alloy 400 by Lead in Secondary Side Steam Generator Environments”, Proc. 7th International Symposium on Environmental Degradation of Materials, NACE, pp. 209-217, 1995.